Metabolomic Markers of Colorectal Tumor With Different Clinicopathological Features

Zhiping Long [1†], Junde Zhou [2†], Kun Xie [1], Zhen Wu [1], Huihui Yin [1], Volontovich Daria [1], Jingshen Tian [1], Nannan Zhang [1], Liangliang Li [1], Yashuang Zhao [1], Fan Wang [1*], Maoqing Wang [3*] and Yunfu Cui [4*]

[1] Department of Epidemiology, School of Public Health, Harbin Medical University, Harbin, China, [2] Department of Colorectal Surgery, The Second Affiliated Hospital of Harbin Medical University, Harbin, China, [3] Department of Nutrition and Food Hygiene, School of Public Health, Harbin Medical University, Harbin, China, [4] Department of General Surgery, The Second Affiliated Hospital of Harbin Medical University, Harbin, China

Background: Colorectal cancer (CRC) is the result of complex interactions between the tumor's molecular profile and metabolites produced by its microenvironment. Despite recent studies identifying CRC molecular subtypes, a metabolite classification system is still lacking. We aimed to explore the distinct phenotypes and subtypes of CRC at the metabolite level.

Methods: We conducted an untargeted metabolomics analysis of 51 paired tumor tissues and adjacent mucosa using ultra-performance liquid chromatography/quadrupole time-of-flight mass spectrometry. Multivariate analysis including principal component analysis, orthogonal partial least squares discriminant analysis and heat maps, univariate analysis, and pathway analysis were used to identify potential metabolite phenotypes of CRC. Unsupervised consensus clustering was used to identify robust metabolite subtypes, and evaluated their clinical relevance.

Results: A total of 173 metabolites (including nucleotides, carbohydrates, free fatty acids, and choline) were identified between CRC tumor tissue and adjacent mucosa. We found that lipid metabolism was closely related to the occurrence and progression of CRC. In particular, CRC tissues could be divided into three subtypes, and statistically significant correlations between different subtypes and clinical prognosis were observed.

Conclusions: CRC tumor tissue exhibits distinct metabolite phenotypes. Metabolite differences between subtypes may provide a basis and direction for further clinical individualized treatment planning.

Keywords: metabolomics, subtypes, CRC, prognosis, lipid metabolism

INTRODUCTION

Colorectal cancer (CRC) is one of the leading causes of cancer-related death, both in China and worldwide. More than one million individuals develop CRC every year and most patients are diagnosed at advanced stages that correspond to poor prognosis (1). With the advances in the treatment of CRC over the past 20 years, median overall survival has been steadily increasing (2). Although the progress made thus far is encouraging, the existing treatment paradigm usually

employs a "one-size-fits-all" approach based on the histopathological diagnosis of CRC, which translates into demonstrable clinical benefit from any given chemotherapeutic regimen in only a small subset of treated patients (3).

It is now being increasingly realized that CRC is not a single disease entity, but a heterogeneous group of tumors, both at the inter-tumoral and intra-tumoral level (2). A major hallmark of CRC is its association with various types of etiological factors and its high heterogeneity in clinical presentation and underlying tumor biology (4). Consequently, most patients with CRC are refractory to treatment and have a dismal outcome. One of the essential requirements to improve their outcome is to provide biomarkers that are capable of accurately defining homogenous molecular subtypes; each displays unique tumor biology linked to potentially druggable driver genes to implement rational treatment choices (5).

Nowadays, tumor genomic profiling is routinely used to classify tumor types, identify driver or germline mutations, perform prognostic assessments, and make therapeutic decisions (6, 7). However, the notable heterogeneity of genomes in cancer tissues makes it difficult to determine the underlying causes or ascertain the optimal treatment. Furthermore, the elevated number of mutations and multiple combinations of tumor suppressors and oncogenes make individualized tumor classification or customized therapy almost impossible (8). Metabolomics is a rapidly growing field of study that endeavors to measure the complete set of metabolites (generally considered to be the intermediates and products of cellular metabolism <1 kDa in size) within a biological sample (that is, the metabolome) to achieve a global view of the state of the system (9). In general, multiple biochemical pathways are affected, owing to the fact that as cancer progresses, multiple defects in biochemical pathways arise as cancer subverts normal metabolism in an effort to survive (10). Furthermore, the metabolite requirements of cancer cells are different from those of most normal differentiated cells, exhibiting different metabolite phenotypes (11). Using metabolomics to identify the specific metabolite subtype of a particular tumor would enable better customization or informed adjustment of cancer therapies (12).

To present, metabolomics-based CRC phenotypic research and molecular typing have been rarely described, and little is known about how changes in metabolite levels relate to the characteristics of tumor tissue. In this study, we described a metabolomics analysis of CRC tissue samples from a group of CRC patients with different clinicopathological features. We aimed to analyze the differential metabolism of tumor tissues with different clinicopathological features, and to explore molecular typing methods for CRC based on metabolomics markers.

Abbreviations: CRC, colorectal cancer; ESI–, negative electrospray ionization; ESI+, positive electrospray ionization; VIP, variable important for the projection; mClusters, metabolite clusters; FFA, free fatty acids; ANIT, adjacent non-involved tissues.

METHODS

Study Design and Subject Recruitment

We designed a self-control study to detect the differential metabolites between tumor tissue and adjacent non-malignant mucosa tissue. Fifty-one pairs of tissue were obtained from surgical resection of CRC patients.

All patients were diagnosed and recruited at the Third Affiliated Hospital of Harbin Medical University. Any patients with neuroendocrine carcinoma, malignant melanoma, non-Hodgkin's lymphoma, gastrointestinal stromal tumors, and Lynch syndrome CRC were excluded. Only newly diagnosed histopathologically confirmed cases were retained. Tissue sampling included the deepest infiltration of the tumor and the adjacent non-malignant mucosa tissues. All tissues were immediately soaked in formaldehyde solution until use.

All procedures performed in studies involving human participants were in accordance with the ethical standards of the Human Research and Ethics Committee of Harbin Medical University and with the 1964 Helsinki declaration and its later amendments or comparable ethical standards. Informed consent was obtained from all individual participants included in the study.

Metabolite Profiling

A detailed description of the experimental protocol of metabolite profiling analysis by UPLC/Q-TOF-MS/MS and the data processing, multivariate and univariate analysis of metabolites, as well as identification of differential metabolites, are provided in the **Supplementary Materials**.

Pathway Analysis

Using an accurate m/z search under 50 ppm, metabolites from positive and negative ionization were matched in Mummichog software, which included metabolites from KEGG and other databases. Mummichog software (version 1.0.9) was used to further test pathway enrichment patterns using permutations, and to compute the probability for each pathway (13).

Metabolite Clustering

Consensus clustering (cCluster; hierarchical clustering; Pearson distance; complete linkage; 1,000 resampling iteration) and unsupervised hierarchical clustering were performed to define subtypes of CRC tumor tissue samples (14, 15). Heatmaps were generated using the Complex Heatmap package in R to determine the relationship among samples or cCluster-defined subgroups (16).

Clinical Relevance Analysis of Metabolite Subtypes

We assessed whether the metabolite subtypes had significant associations with overall survival. The R packages "survival" and "survminer" were used to perform the overall survival analysis and to produce Kaplan-Meier survival plots. A log-rank test was used to assess the significance ($P < 0.05$). We further assessed whether the metabolite subtypes remained significantly associated with overall survival after adjusting for age, sex,

clinical stage, postoperative chemotherapy, and immunotherapy as covariates in the Cox model.

RESULTS

Metabolite Profiling of 51 Pairs of Tumor Tissue and Adjacent Mucosa Tissue

To identify the differential metabolites of CRC, the metabolomes of tumor tissues were compared with that of matched adjacent mucosa. **Supplementary Table 1** shows the demographic characteristics and clinicopathological features of 51 CRC patients. Mass spectrometry detected 4,526 and 4,765 variables in negative electrospray ionization (ESI-) and positive electrospray ionization (ESI+), respectively. Multivariate analysis was performed on the result of mass spectrometry to find metabolites that mostly discriminated the study groups. Principal component analysis (PCA) was the unsupervised analysis method, which was used for dimension reduction of data through making a linear combination of variables known as principal components. PCA analysis can reveal trends in the data and groups of observations and find outliers. Although a weak trend in clustering according to the PCA plot based on tumor tissue and adjacent mucosa was observed, the PCA analysis results showed a separation of tumor tissue and adjacent mucosa into two clusters (**Figures 1A,D**). To further study the differences between tumor tissue and adjacent mucosa and to find potential biomarkers, the supervised multivariate statistical method OPLS-DA was subsequently used. OPLS-DA is a supervised analysis method that is employed to divide the samples into different groups, including tumor tissue and adjacent mucosa, which was performed to find metabolites that mostly discriminated the studied groups in each comparison. The classification results are shown in **Figures 1B,E**. To guard against model overfitting, permutation tests (100 random permutations) were performed. These permutation tests were used to contrast the goodness of fit of the original model with the goodness of fit of randomly permuted models. As shown in **Figures 1C,F**, the validation plots strongly indicated that the original combined models were valid. No overfitting was observed.

A total of 373 metabolites (296 higher and 77 lower) were identified with the criteria of Variable important for the projection (VIP) score >1.5 and P-values of <0.05 in the false detection rate (FDR)-corrected Mann-Whitney U tests, which displayed differential abundance between tumor and adjacent mucosa samples (**Supplementary Figure 1**). The Human Metabolome Database (http://www.hmdb.ca/) mass search feature was used as to aid metabolite identification. A total of 173 metabolites were identified as shown in **Supplementary Table 2**. Interestingly, nucleotides, carbohydrates, free fatty acids, and choline were overrepresented and highly abundant in tumors, such as D-ribulose 5-phosphate, D-glucose, xylulose 5-phosphate, 3'-AMP, hypoxanthine, palmitoleic acid, and cytidine monophosphate (**Supplementary Table 2**).

Metabolite Landscape of CRC Tumors

Pathway analysis was performed to systematically investigate the metabolite alterations associated with CRC pathogenesis.

Mummichog software, a pathway tool designed for untargeted metabolomics data [13], was used to evaluate the significant metabolite pathways utilizing metabolites that were present at differential abundance between CRC tissues and adjacent mucosa. The mummichog analysis was performed on the previously identified 373 positive and negative ions, and the results are shown in **Supplementary Table 3**; interestingly, among the 34 metabolite pathways, most were involved in lipid metabolism ($n = 7$) and glycan biosynthesis and metabolism ($n = 8$). Other metabolite pathways included glycolysis/gluconeogenesis, pentose phosphate pathway, and tryptophan metabolism.

Metabolite Changes Upon CRC Progression

Difference stage-distributed CRC samples allowed us to investigate the association between metabolite shifts and CRC progression. Based on the 4,526 and 4,765 variables in ESI– and ESI+, using American Joint Committee on Cancer (AJCC) clinical staging, the OPLS-DA analysis of the metabolite profiles of tumor tissue could separate clusters for each stage (**Figure 2**). Validation of the OPLS-DA model was performed here by permutation testing. Although the permutation test indicates that the OPLS-DA model is valid, the model fitting is not very satisfactory (**Supplementary Figure 2**). There were 94 metabolites exhibiting statistically significant differential abundance between early-(I, II) and late-stage (III, IV) tumors (VIP > 1.5 and Mann-Whitney U-test FDR corrected P-value < 0.01), and a total of 48 metabolites were identified (**Supplementary Table 3**). Most lipid metabolites showed an increase in late-stage tumors, while dipeptides also showed a decrease in late-stage tumors (**Supplementary Figure 3**). The results of pathway analysis by Mummichog software indicated that significant features are enriched for pathways involved in lipid metabolism (**Supplementary Table 4**).

Metabolite Alterations of CRC Pathologic Characteristics

We also sought to determine whether we could identify the differences in metabolite features among various histopathological classifications of CRC. The separation of adenocarcinoma and non-adenocarcinoma CRCs was observed using OPLS-DA (**Figure 3**). Similarly, the permutation test indicates that the OPLS-DA model is valid, but, the model fitting is also unsatisfactory (**Supplementary Figure 4**). Forty-three metabolites exhibited statistically significant differential abundance between adenocarcinoma and non-adenocarcinoma tumors (VIP > 1.5 and P < 0.01). Furthermore, a total of 26 metabolites were identified (**Supplementary Table 5**) and almost all these 26 metabolites were lipids. Mummichog indicated that pathways involved in lipid metabolism were also significantly enriched (**Supplementary Table 5**).
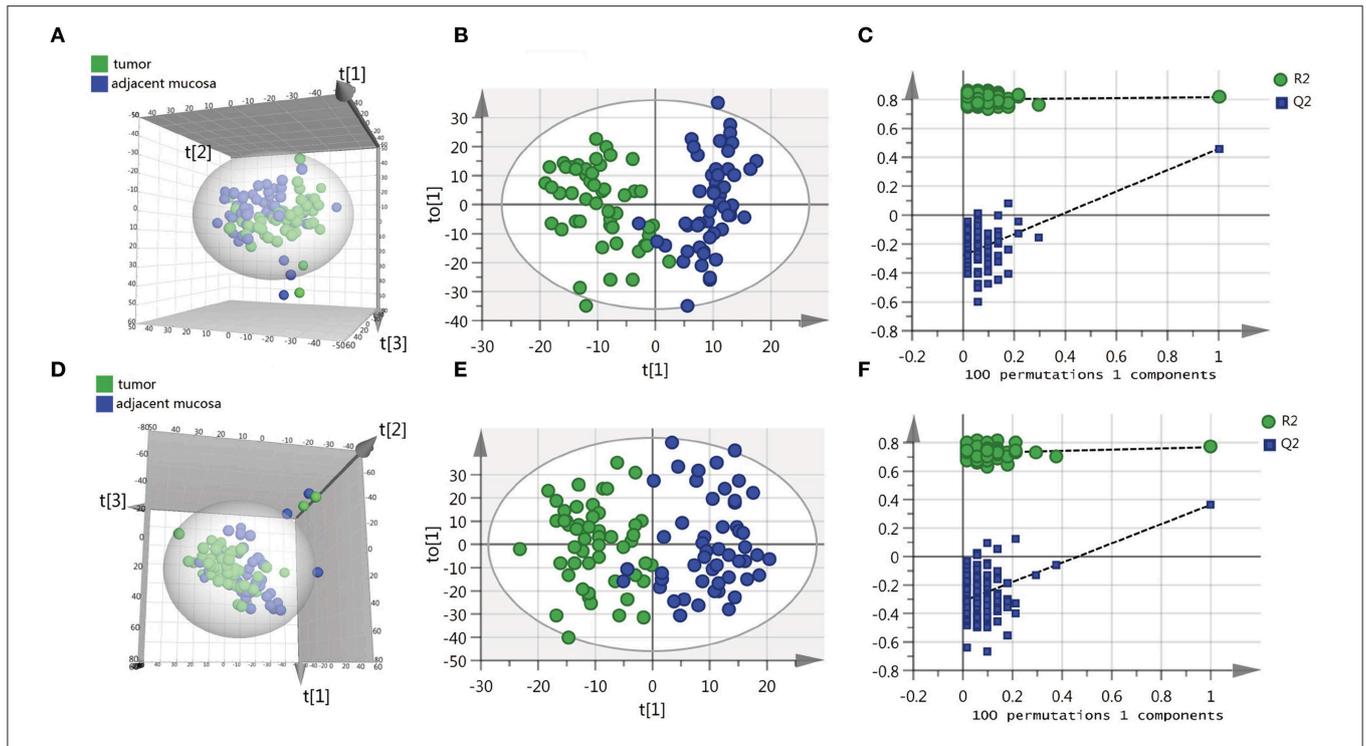
FIGURE 1 | Scatter score plots of the PCA and OPLS-DA model based on the tumor tissue vs. adjacent mucosa data set and their corresponding score plots of 100 permutations. **(A)** PCA score plot in ESI⁻ model, $R^2X = 0.529$, $Q^2 = 0.284$. **(B)** OPLS-DA score plot in ESI⁻ model, $R^2X = 0.218$, $R^2Y = 0.817$, $Q^2 = 0.459$. **(C)** Permutation test result of the OPLS-DA model in ESI⁻ model; **(D)** PCA score plot in ESI⁺ model, $R^2X = 0.587$, $Q^2 = 0.316$. **(E)** OPLS-DA score plot in ESI⁺ model, $R^2X = 0.246$, $R^2Y = 0.768$, $Q^2 = 0.364$. **(F)** Permutation test result of the OPLS-DA model in ESI⁺ model. t[1], t[2], t[3] and to[1] represent the first predicted principal component (X axis), second predicted principal component (Y axis), third predicted principal component (Z axis) and first orthogonal component; The criteria for validity are: all blue Q2-values to the left are lower than the original points to the right, or the blue regression line of the Q2-points intersects the vertical axis (on the left) at, or below zero.
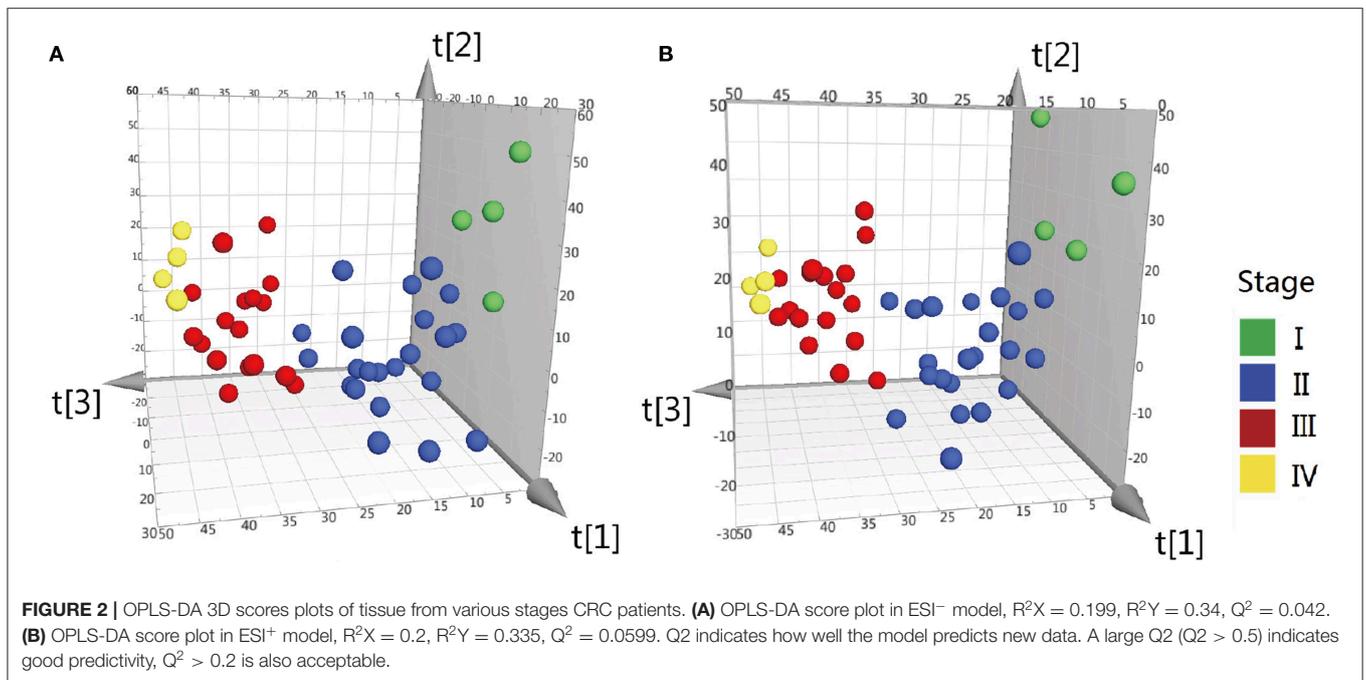

FIGURE 2 | OPLS-DA 3D scores plots of tissue from various stages CRC patients. **(A)** OPLS-DA score plot in ESI⁻ model, $R^2X = 0.199$, $R^2Y = 0.34$, $Q^2 = 0.042$. **(B)** OPLS-DA score plot in ESI⁺ model, $R^2X = 0.2$, $R^2Y = 0.335$, $Q^2 = 0.0599$. Q2 indicates how well the model predicts new data. A large Q2 (Q2 > 0.5) indicates good predictivity, $Q^2 > 0.2$ is also acceptable.

FIGURE 3 | OPLS-DA score plots of tissue from various histopathologic classification CRC patients. **(A)** OPLS-DA score plot in ESI$^-$ model, $R^2X = 0.088$, $R^2Y = 0.876$, $Q^2 = 0.128$. **(B)** OPLS-DA score plot in ESI$^+$ model, $R^2X = 0.229$, $R^2Y = 0.984$, $Q^2 = -0.026$.
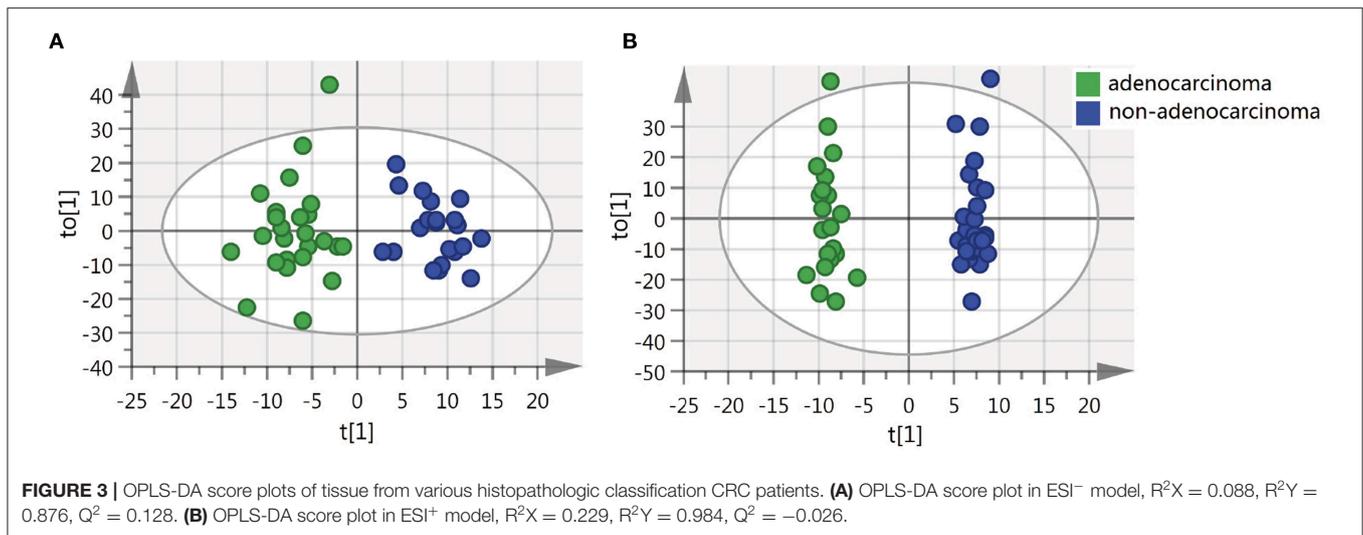
Unsupervised Clustering Reveals Three Metabolite Clusters (mClusters) With Prognostic Value

The results of cCluster showed that CRC tumor samples can be partitioned into clusters with distinct metabolite phenotypes using the differential metabolites among tumor and adjacent mucosa samples. cCluster revealed three major subtypes of CRC according to consensus distributions and the corresponding consensus matrices (**Figure 4**). Especially, the CRC subtypes defined by cCluster can be obviously observed through unsupervised hierarchical clustering (**Figure 5**), which is much clearer than the classification effect according to the pathological stages of tumor in **Supplementary Figure 3**. The rough estimate by chi-square tests indicated that there was no statistically significant consistency between the three mClusters and clinicopathological features, respectively (as shown in **Figure 5**). This analysis revealed unique subtypes of CRC cases with distinct metabolite patterns that were independent of known clinicopathological features.

For each metabolite cluster (mCluster), the clinical stages at presentation are summarized in **Supplementary Figure 5**. mCluster 1 had the highest percentage (66.7%) of early-stage (I & II) tumors and was characterized by the low abundance of carbohydrates, nucleotide metabolites, dipeptides, and lipids; mCluster 2 had the highest percentage (51.9%) of late-stage (III & IV) tumors and displayed medium levels of all metabolites; mCluster 3, characterized by the highest abundance of carbohydrates, nucleotide metabolites, dipeptides, and lipids, accounted for 62.5% early-stage tumors (**Figure 5** and **Supplementary Figure 5**).
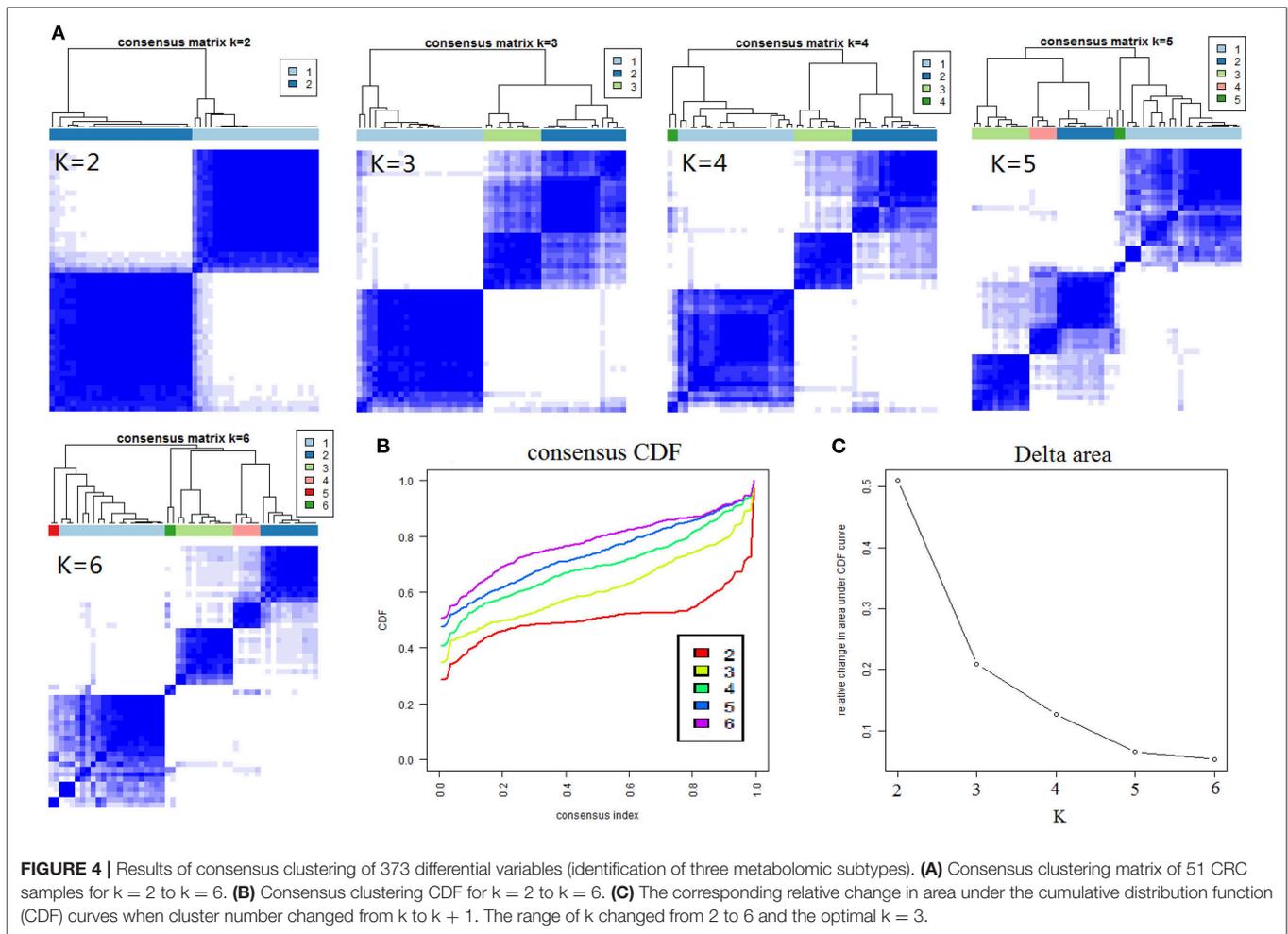
Additionally, we further determined the correlations of mClusters with patients' overall survival. As shown in **Figure 6A**, the result did not reach statistical significance, likely due to the relatively small number of events during follow-up (log-rank $P = 0.099$). However, regardless of clinical staging, mCluster 1 and 3 (the two groups with similar prognostic survival) were combined,

cases defined as mCluster 2 showed statistically significant poor survival (log-rank $P = 0.032$, **Figure 6B**). More importantly, we obtained the same results using Cox regression models adjusting by age, sex, clinical stage, and postoperative chemotherapy and immunotherapy ($P = 0.027$, **Figure 6C**).

DISCUSSION

Metabolomics analysis of CRC can not only distinguish tumor tissue from adjacent mucosa, but can also discriminate CRC patients with different clinicopathological features. What's more, through the high-throughput metabolomics analysis using UPLC/Q-TOF MS mass spectrometry platform, metabolite profiling allows a more comprehensive understanding of CRC phenotyping. We are the first time defined molecular subtypes of CRC based on metabolomics. The results of our study indicated the molecular subtyping based on differential metabolites showed much better classification effect than according to pathological stages of tumor; especially, significant differences in survival was observed of the metabolic subtypes. It suggested us individualized treatment guided by molecular typing based on metabolites may be more reasonable and effective than treatment based on the same stage or morphological type.

Tian et al. analyzed the metabonomic signatures of 50 human CRC tissues and their adjacent non-involved tissues (ANIT) using high-resolution magic-angle spinning (HRMAS) 1H NMR spectroscopy together with the fatty acid compositions of these tissues using GC-FID/MS (17). In this study, metabonomic phenotypes of CRC tissues differed significantly from that of ANIT in energy metabolism, membrane biosynthesis and degradation, and osmotic regulation together with the metabolism of proteins and nucleotides. Diverse metabolite pathways including N-glycan biosynthesis and degradation, linoleate metabolism, leukotriene metabolism, butanoate metabolism, glycosphingolipid biosynthesis, drug metabolism-cytochrome P450 and vitamin B5-CoA biosynthesis from

FIGURE 4 | Results of consensus clustering of 373 differential variables (identification of three metabolomic subtypes). **(A)** Consensus clustering matrix of 51 CRC samples for k = 2 to k = 6. **(B)** Consensus clustering CDF for k = 2 to k = 6. **(C)** The corresponding relative change in area under the cumulative distribution function (CDF) curves when cluster number changed from k to k + 1. The range of k changed from 2 to 6 and the optimal k = 3.

pantothenate significantly differed between tumor and normal tissues. The UPLC/Q-TOF MS-based metabolomics approach of this study provided additional information that complements our current understanding of the metabolomic characteristics between CRC tumor tissues and adjacent mucosa.

The Warburg effect is a known feature of cancer metabolism that describes maintenance of a high aerobic glycolysis rate and high levels of glucose uptake and lactate production during tumor growth (18, 19). Our findings are consistent with the Warburg effect. The difference in energy metabolism can be clearly observed between CRC tumor tissues and adjacent mucosa. Compared with adjacent mucosa, carbohydrates in colorectal cancer tissues were significantly increased and the pentose phosphate pathway and glycolysis/gluconeogenesis pathways were identified. In cancer metabolism, glycolysis is the preferred pathway to produce metabolite intermediates used to support cell proliferation during *de novo* biosynthesis (20), which can lead to higher levels of free fatty acids (FFA) and nucleic acid-related metabolites. In our current study, higher levels of nucleotides, palmitoleic acid, and hypoxanthine were observed in tumor tissues. Nucleotides are critical components of DNA and RNA structures, and disorders in their biosynthesis

have profound effects on cell physiology, which may lead to tumor transformation in cells (21). CRC tumor tissues showed higher levels of choline metabolites such as choline, PC, and PE than adjacent mucosa, which have also been reported in other malignancies (22–24).

Glycosylation changes are some of the most common post-translational modifications of proteins and are considered markers of cancer. N-glycans can regulate cell migration, cell adhesion, cell signaling, proliferation, and metastasis. Many carbohydrate-mediated cellular mechanisms, including those important for tumor progression, are regulated by N-glycans (25). Stephanie et al. compared the glycosylation profiles of tumor tissues and corresponding control tissues in 13 CRC patients (26). Multivariate data analysis showed significant differences in glycosphingolipids between tumors and corresponding adjacent tissues using MALDI-TOF(/TOF)-MS and 2-dimensional LC-MS/MS; the main changes included elevated fucosylation, reduced acetylation and sulfation, and reduced expression of globular glycans, as well as disialyl gangliosides. In our study, seven metabolite pathways were identified as being involved in the biosynthesis and metabolism of glycans, including biosynthesis of N-glycans, degradation of N-glycans, and
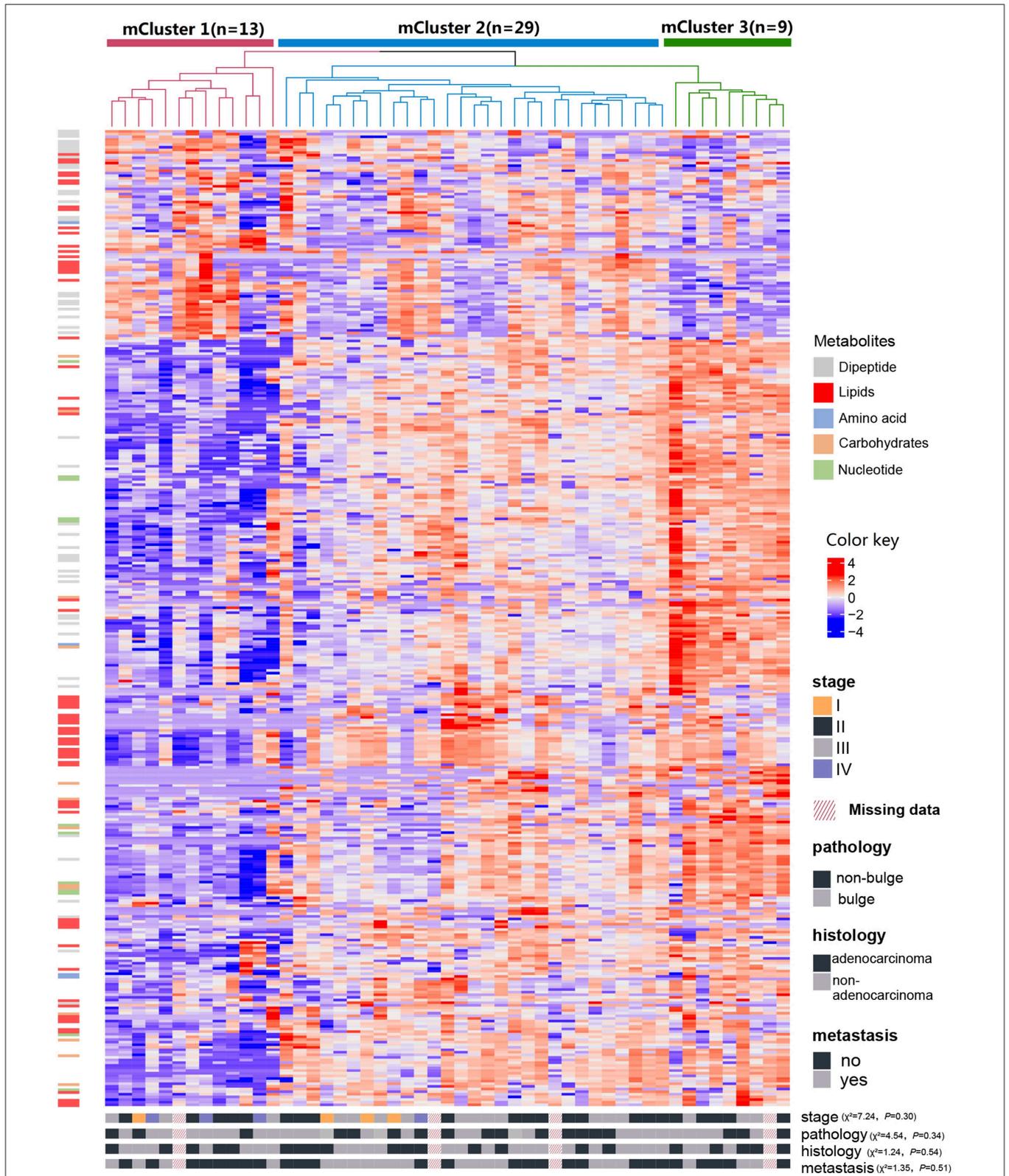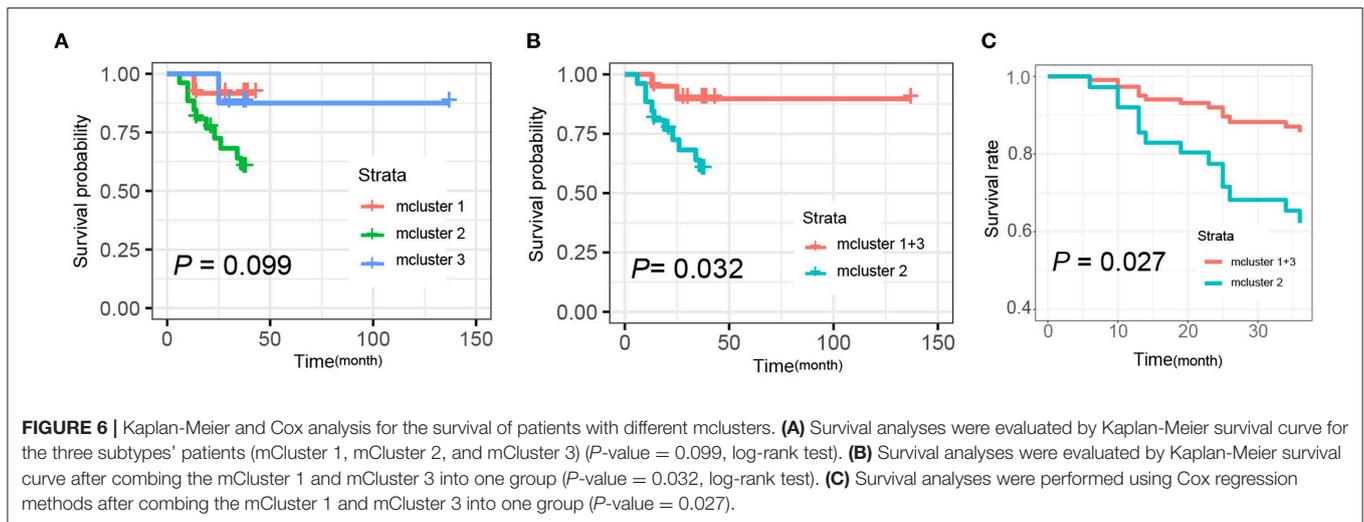
FIGURE 5 | Identification of CRC metabolite-based tumor subtypes. A heatmap of CRC subtypes is shown based on consensus clustering. The x-axis represents CRC subtype consensus clusters. CRC samples are represented in columns, grouped by the dendrogram into three main clusters, and metabolites ($n = 373$) are represented in rows. Clinical data of the samples are included below the heatmap and the chi-square tests were used to estimate the difference between the three mClusters and clinicopathological features, respectively.

FIGURE 6 | Kaplan-Meier and Cox analysis for the survival of patients with different mclusters. **(A)** Survival analyses were evaluated by Kaplan-Meier survival curve for the three subtypes' patients (mCluster 1, mCluster 2, and mCluster 3) (*P*-value = 0.099, log-rank test). **(B)** Survival analyses were evaluated by Kaplan-Meier survival curve after combing the mCluster 1 and mCluster 3 into one group (*P*-value = 0.032, log-rank test). **(C)** Survival analyses were performed using Cox regression methods after combing the mCluster 1 and mCluster 3 into one group (*P*-value = 0.027).

metabolism and biosynthesis of glycosphingolipids, confirming the changes in characteristic tumor-associated glycosylation.

To date, there have been few studies analyzing the differences in the metabolism of CRC with different clinicopathological features. In this study, it was reported for the first time that the early tumors of CRC have higher abundance of dipeptide characteristics. A large increase in dipeptides may be produced through protein degradation/reutilization processes, such as lysosomal degradation, phagocytosis, endocytosis, pinocytosis, and autophagy (27–30). Brauns et al. (31) have shown that cyclic dipeptides, especially those containing proline, have important biological activities. Their results indicated that phenylalanine–proline inhibits the proliferation of HT-29, MCF-7, and HeLa cells, as well as inducing apoptosis in HT-29 colon cancer cells, which has potential anti-tumor activity (31).

Higher levels of lipid metabolites observed in the current study in advanced CRC tissues have been reported in other studies (17, 32). Results of the Mummichog software pathway analysis showed that most pathways are lipid metabolism-related, consistent with previous studies by Zhang et al. and Tian et al. (17, 33). Abnormal lipid metabolism is a metabolite marker of cancer cells (34, 35), and many studies have reported that cancer cells have strong lipid and cholesterol affinities (35), by activating the exogenous (or dietary) lipid and lipoprotein uptake or by enhancing the reticular fat from the cytosol acetyl-CoA Biosynthesis of cholesterol and cholesterol, highly proliferative. Changes in lipid metabolism in CRC tumor tissues suggest enhanced lipogenesis is one of the most important features in CRC tumor tissues (36). Recent studies have also found that tumor tissue can use fatty acids and lipolytic pathways to obtain fatty acids to promote tumor cell proliferation (37).

We further observed that the metabolite differences between adenocarcinoma and non-adenocarcinoma CRCs were mainly related to lipid metabolism. Lipid metabolism is regulated by complex signaling networks in CRC tumor cells, which are closely related to cell growth, proliferation, differentiation, survival, and apoptosis (38). Several studies have indicated that some fatty acid metabolism pathways are associated with the development and progression of colorectal adenocarcinoma (39, 40). Beatriz et al. also showed that changes in fatty acid metabolism are a crucial factor in the progression from colorectal adenoma to adenocarcinoma (41). Although our results are consistent with previous studies, there have been no studies on the metabolite differences of adenocarcinoma and non-adenocarcinoma thus far.

TNM staging system is currently recognized as an important independent indicator that can comprehensively reflect the progress of malignant tumor and judge the prognosis. It is also the main basis for determining the surgical resection scope, surgical method and formulation of adjuvant treatment plan. But, limitations cannot be ignored. TNM staging was determined based on the depth of invasion, lymph node metastasis and distant metastasis of the tumor in the intestinal wall. The essence of TNM staging is the clinical observable morphological index of the invasion and metastasis ability and degree of tumor, as well as adenocarcinoma and non-adenocarcinoma. Some recent studies have also indicated that, based on TNM staging and histological features, the sensitivity and prognosis of the same group of patients to the same treatment regimen vary greatly (42).

Our results, for the first time, showed that CRC could be divided into three subtypes at the metabolomics level, and the heterogeneity of metabolomic changes between different subtypes lead to inconsistent prognosis of tumors. Lipids, nucleotides, and carbohydrates have important roles in the biology of a subset of tumors. The differences in these metabolite levels between subtypes may point to different pathophysiological mechanisms for the development and progression of CRC. Understanding the pathogenesis of CRC is critical to developing personalized treatment strategies. As every CRC covers a specific, heterogeneous metabolite profile, the question rises if metabolomics (and other "omics") approaches could become the new standard in adequately categorizing CRC on a molecular basis. This molecular classification could offer patients

a personalized therapy schedule, depending on the type of molecular defects that their colorectal tumor has acquired.

For example, many anticancer drugs are based on lipid metabolism, such as irinotecan, which can affect the accumulation of ceramide by inducing ceramide synthase to catalyze ceramide synthesis or by activating sphingomyelinase to catalyze the degradation of sphingomyelin (43, 44). At the same time, the use of drugs is also dependent on the sensitivity and intrinsic drug resistance of cancer cells. Studies have shown that omega-3 polyunsaturated fatty acids can improve the efficacy of chemotherapy and radiotherapy. Omega-3 fatty acids also reduce CD133+ colon cancer stem cell-like cells markers and increase sensitivity to chemotherapy (45). A eicosapentaenoic acid-free fatty acid(EPA-FFA) phase II double-blind, placebo-controlled trial of patients undergoing liver resection for CRC liver metastases showed that EPA-FFA treatment is anti-angiogenic, safe, and well tolerated (46). Backshall et al. evaluate the effect of pretreatment serum metabolite profiles generated by 1H NMR spectroscopy on toxicity in patients with inoperable CRC receiving single agent capecitabine (47). Their study suggests that metabolite profiles can delineate subpopulations susceptible to adverse events and have a potential role in the assessment of treatment viability for cancer patients prior to commencing chemotherapy.

This study still has some limitations. Our study is based on a relatively small sample of CRC patients in northeastern China. Tissue samples of patients with CRC are based on the continuous collection of clinical cases in the same hospital; the selection of samples may be biased. Moreover, the UPLC/Q-TOF MS metabolomics platform used in the study was used in isolation and some metabolites may not have been detected. Therefore, confirmation is necessary based on large samples from multiple populations and platforms.

In summary, our metabolomics study indicates that CRC tumor tissue exhibits distinct metabolite phenotypes. Metabolomics provides a new window into the study of CRC phenotypes and molecular typing as CRC can be divided into three subtypes at the metabolite level. When integrated with other platforms, we can provide a more comprehensive explanation of the complex biology associated with CRC and malignant transformation. A deeper understanding of abnormal metabolism will provide a framework for the design and implementation of personalized approaches to CRC treatment through metabolite regulation.

DATA AVAILABILITY STATEMENT

The datasets presented in this study can be found in online repositories. The names of the repository/repositories and accession number(s) can be found below: FigShare (https://doi.org/10.6084/m9.figshare.12311315).

ETHICS STATEMENT

The studies involving human participants were reviewed and approved by the Ethics Committee of Harbin Medical University. The patients/participants provided their written informed consent to participate in this study.

AUTHOR CONTRIBUTIONS

All authors listed have made a substantial, direct and intellectual contribution to the work, and approved it for publication.

FUNDING

SUPPLEMENTARY MATERIAL

The Supplementary Material for this article can be found online at: https://www.frontiersin.org/articles/10.3389/fonc.2020.00981/full#supplementary-material

REFERENCES

1. Siegel RL, Miller KD, Jemal A. Cancer statistics, 2018. *CA Cancer J Clin.* (2018) 68:7–30. doi: 10.3322/caac.21442
2. Kuipers EJ, Grady WM, Lieberman D, Seufferlein T, Sung JJ, Boelens PG, et al. Colorectal cancer. *Nat Rev Dis Primers.* (2015) 1:15065. doi: 10.1038/nrdp.2015.65
3. Goel G. Molecular characterization and biomarker identification in colorectal cancer: Toward realization of the precision medicine dream. *Cancer Manag Res.* (2018) 10:5895–908. doi: 10.2147/CMAR.S162967
4. Cunningham D, Atkin W, Lenz HJ, Lynch HT, Minsky B, Nordlinger B, et al. Colorectal cancer. *Lancet.* (2010) 375:1030–47. doi: 10.1016/S0140-6736(10)60353-4
5. Guinney J, Dienstmann R, Wang X, de Reyniès A, Schlicker A, Soneson C, et al. The consensus molecular subtypes of colorectal cancer. *Nat Med.* (2015) 21:1350–6. doi: 10.1038/nm.3967
6. Chaisaingmongkol J, Budhu A, Dang H, Rabibhadana S, Pupacdi B, Kwon SM, et al. Common molecular subtypes among asian hepatocellular carcinoma and cholangiocarcinoma. *Cancer Cell.* (2017) 32:57–70.e3. doi: 10.1016/j.ccell.2017.05.009
7. Choi W, Ochoa A, McConkey DJ, Aine M, Höglund M, Kim WY, et al. Genetic alterations in the molecular subtypes of bladder cancer: illustration in the cancer genome atlas dataset. *Eur Urol.* (2017) 72:354–65. doi: 10.1016/j.eururo.2017.03.010
8. Forbes SA, Beare D, Gunasekaran P, Leung K, Bindal N, Boutselakis H, et al. COSMIC: exploring the world's knowledge of somatic mutations in human cancer. *Nucleic Acids Res.* (2015) 43(Database issue):D805–11. doi: 10.1093/nar/gku1075
9. Johnson CH, Ivanisevic J, Siuzdak G. Metabolomics: beyond biomarkers and towards mechanisms. *Nat Rev Mol Cell Biol.* (2016) 17:451–9. doi: 10.1038/nrm.2016.25
10. Vander Heiden MG, DeBerardinis RJ. Understanding the intersections between metabolism and cancer biology. *Cell.* (2017) 168:657–69. doi: 10.1016/j.cell.2016.12.039

11. Levine AJ, Puzio-Kuter AM. The control of the metabolic switch in cancers by oncogenes and tumor suppressor genes. *Science.* (2010) 330:1340–4. doi: 10.1126/science.1193494

12. Wishart DS. Is cancer a genetic disease or a metabolic disease? *EBioMedicine.* (2015) 2:478–9. doi: 10.1016/j.ebiom.2015.05.022

13. Li S, Park Y, Duraisingham S, Strobel FH, Khan N, Soltow QA, et al. Predicting network activity from high throughput metabolomics. *PLoS Comp Biol.* (2013) 9:e1003123. doi: 10.1371/journal.pcbi.1003123

14. Monti S, Savage KJ, Kutok JL, Feuerhake F, Kurtin P, Mihm M, et al. Molecular profiling of diffuse large B-cell lymphoma identifies robust subtypes including one characterized by host inflammatory response. *Blood.* (2005) 105:1851–61. doi: 10.1182/blood-2004-07-2947

15. Wilkerson MD, Hayes DN. ConsensusClusterPlus: a class discovery tool with confidence assessments and item tracking. *Bioinformatics.* (2010) 26:1572–3. doi: 10.1093/bioinformatics/btq170

16. Gu Z, Eils R, Schlesner M. Complex heatmaps reveal patterns and correlations in multidimensional genomic data. *Bioinformatics.* (2016) 32:2847–9. doi: 10.1093/bioinformatics/btw313

17. Tian Y, Xu T, Huang J, Zhang L, Xu S, Xiong B, et al. Tissue metabonomic phenotyping for diagnosis and prognosis of human colorectal cancer. *Sci Rep.* (2016) 6:20790. doi: 10.1038/srep20790

18. Warburg O. [Origin of cancer cells]. *Oncologia.* (1956) 9:75–83. doi: 10.1159/000223920

19. Gatenby RA, Gillies RJ. Why do cancers have high aerobic glycolysis? *Nat Rev Cancer.* (2004) 4:891–9. doi: 10.1038/nrc1478

20. Vander Heiden MG, Cantley LC, Thompson CB. Understanding the Warburg effect: the metabolic requirements of cell proliferation. *Science.* (2009) 324:1029–33. doi: 10.1126/science.1160809

21. Tong X, Zhao F, Thompson CB. The molecular determinants of de novo nucleotide biosynthesis in cancer cells. *Curr Opin Genet Dev.* (2009) 19:32–7. doi: 10.1016/j.gde.2009.01.002

22. Chan EC, Koh PK, Mal M, Cheah PY, Eu KW, Backshall A, et al. Metabolic profiling of human colorectal cancer using high-resolution magic angle spinning nuclear magnetic resonance (HR-MAS NMR) spectroscopy and gas chromatography mass spectrometry (GC/MS). *J Proteome Res.* (2009) 8:352–61. doi: 10.1021/pr8006232

23. Chae YK, Kang W-Y, Kim SH, Joo JE, Han JK, Hong BW. Combining information of common metabolites reveals global differences between colorectal cancerous and normal tissues. *Bull Korean Chem Soc.* (2010) 31:379. doi: 10.5012/bkcs.2010.31.02.379

24. Griffin JL, Shockcor JP. Metabolic profiles of cancer cells. *Nat Rev Cancer.* (2004) 4:551. doi: 10.1038/nrc1390

25. de Freitas Junior JCM, Morgado-Díaz JA. The role of N-glycans in colorectal cancer progression: potential biomarkers and therapeutic applications. *Oncotarget.* (2016) 7:19395. doi: 10.18632/oncotarget.6283

26. Holst S, Stavenhagen K, Balog CI, Koeleman CA, McDonnell LM, Mayboroda OA, et al. Investigations on aberrant glycosylation of glycosphingolipids in colorectal cancer tissues using liquid chromatography and matrix-assisted laser desorption time-of-flight mass spectrometry (MALDI-TOF-MS). *Mol Cell Proteomics.* (2013) 12:3081–93. doi: 10.1074/mcp.M113.030387

27. Commisso C, Davidson SM, Soydaner-Azeloglu RG, Parker SJ, Kamphorst JJ, Hackett S, et al. Macropinocytosis of protein is an amino acid supply route in Ras-transformed cells. *Nature.* (2013) 497:633. doi: 10.1038/nature12138

28. Kimmelman AC. Metabolic dependencies in RAS-driven cancers. *AACR.* (2015) 21:1828–34. doi: 10.1158/1078-0432.CCR-14-2425

29. Mizushima N, Komatsu M. Autophagy: renovation of cells and tissues. *Cell.* (2011) 147:728–41. doi: 10.1016/j.cell.2011.10.026

30. Settembre C, Ballabio A. Lysosome: regulator of lipid degradation pathways. *Trends Cell Biol.* (2014) 24:743–50. doi: 10.1016/j.tcb.2014.06.006

31. Brauns SC, Milne P, Naudé R, Van de Venter M. Selected cyclic dipeptides inhibit cancer cell growth and induce apoptosis in HT-29 colon cancer cells. *Anticancer Res.* (2004) 24:1713–20.

32. Liesenfeld DB, Grapov D, Fahrmann JF, Salou M, Scherer D, Toth R, et al. Metabolomics and transcriptomics identify pathway

differences between visceral and subcutaneous adipose tissue in colorectal cancer patients: the ColoCare study. *Am J Clin Nutr.* (2015) 102:433–43. doi: 10.3945/ajcn.114.103804

33. Zhang H, Qiao L, Li X, Wan Y, Yang L, Wang H. Tissue metabolic profiling of lymph node metastasis of colorectal cancer assessed by 1H NMR. *Oncol Rep.* (2016) 36:3436–48. doi: 10.3892/or.2016.5175

34. Glunde K, Bhujwalla ZM, Ronen SM. Choline metabolism in malignant transformation. *Nat Rev Cancer.* (2011) 11:835. doi: 10.1038/nrc3162

35. Beloribi-Djefaflia S, Vasseur S, Guillaumond F. Lipid metabolic reprogramming in cancer cells. *Oncogenesis.* (2016) 5:e189. doi: 10.1038/oncsis.2015.49

36. Zaidi N, Lupien L, Kuemmerle NB, Kinlaw WB, Swinnen JV, Smans K. Lipogenesis and lipolysis: the pathways exploited by the cancer cells to acquire fatty acids. *Progr Lipid Res.* (2013) 52:585–9. doi: 10.1016/j.plipres.2013.08.005

37. Nomura DK, Long JZ, Niessen S, Hoover HS, Ng S-W, Cravatt BF. Monoacylglycerol lipase regulates a fatty acid network that promotes cancer pathogenesis. *Cell.* (2010) 140:49–61. doi: 10.1016/j.cell.2009.11.027

38. Huang C, Freter C. Lipid metabolism, apoptosis and cancer therapy. *Int J Mol Sci.* (2015) 16:924–49. doi: 10.3390/ijms16010924

39. Gassler N, Herr I, Schneider A, Penzel R, Langbein L, Schirmacher P, et al. Impaired expression of acyl-CoA synthetase 5 in sporadic colorectal adenocarcinomas. *J Pathol.* (2005) 207:295–300. doi: 10.1002/path.1831

40. Pakiet A, Kobiela J, Stepnowski P, Sledzinski T, Mika A. Changes in lipids composition and metabolism in colorectal cancer: a review. *Lipids Health Dis.* (2019) 18:29. doi: 10.1186/s12944-019-0977-8

41. Carvalho B, Sillars-Hardebol AH, Postma C, Mongera S, Terhaar Sive Droste J, Obulkasim A, et al. Colorectal adenoma to carcinoma progression is accompanied by changes in gene expression associated with ageing, chromosomal instability, and fatty acid metabolism. *Cell Oncol.* (2012) 35:53–63. doi: 10.1007/s13402-011-0065-1

42. Brenner H, Bouvier AM, Foschi R, Hackl M, Larsen IK, Lemmens V, et al. Progress in colorectal cancer survival in Europe from the late 1980s to the early 21st century: the EUROCARE study. *Int J Cancer.* (2012) 131:1649–58. doi: 10.1002/ijc.26192

43. Saddoughi SA, Ogretmen B. Diverse functions of ceramide in cancer cell death and proliferation. *Adv Cancer Res.* (2013) 117:37–58. doi: 10.1016/B978-0-12-394274-6.00002-9

44. Senchenkov A, Litvak DA, Cabot MC. Targeting ceramide metabolism—a strategy for overcoming drug resistance. *J Natl Cancer Inst.* (2001) 93:347–57. doi: 10.1093/jnci/93.5.347

45. De Carlo F, Witte TR, Hardman WE, Claudio PP. Omega-3 eicosapentaenoic acid decreases CD133 colon cancer stem-like cell marker expression while increasing sensitivity to chemotherapy. *PLoS ONE.* (2013) 8:e69760. doi: 10.1371/journal.pone.0069760

46. Cockbain AJ, Volpato M, Race AD, Munarini A, Fazio C, Belluzzi A, et al. Anticolorectal cancer activity of the omega-3 polyunsaturated fatty acid eicosapentaenoic acid. *Gut.* (2014) 63:1760–8. doi: 10.1136/gutjnl-2013-306445

47. Backshall A, Sharma R, Clarke SJ, Keun HC. Pharmacometabonomic profiling as a predictor of toxicity in patients with inoperable colorectal cancer treated with capecitabine. *Clin Cancer Res.* (2011) 17:3019–28. doi: 10.1158/1078-0432.CCR-10-2474

Conflict of Interest: The authors declare that the research was conducted in the absence of any commercial or financial relationships that could be construed as a potential conflict of interest.